Structural, thermodynamic, and transport properties of aqueous reline and ethaline solutions from Molecular Dynamics Simulations

Celebi, Alper T.; Vlugt, Thijs J.H.; Moultos, Othonas A.

DOI
10.1021/acs.jpcb.9b09729

Publication date
2019

Document Version
Final published version

Published in
Journal of Physical Chemistry B

THE JOURNAL OF PHYSICAL CHEMISTRY B

Article

Cite This: J. Phys. Chem. B 2019, 123, 11014−11025

pubs.acs.org/JPCB

Structural, Thermodynamic, and Transport Properties of Aqueous Reline and Ethaline Solutions from Molecular Dynamics Simulations

Alper T. Celebi, Thijs J. H. Vlugt, and Othonas A. Moultos*

Engineering Thermodynamics, Process & Energy Department, Faculty of Mechanical, Maritime and Materials Engineering, Delft University of Technology, Leeghwaterstraat 39, 2628CB Delft, The Netherlands

Supporting Information

ABSTRACT: Deep eutectic solvents (DESs) are a new generation of green solvents, which are considered an environmentally friendly alternative to ionic liquids and volatile organic compounds. The addition of controlled amounts of water to DESs has a significant effect on their microscopic structure and thus on their thermodynamic and transport properties. In this way, DESs can be modified, leading to solvents with improved characteristics. In this work, molecular dynamics (MD) simulations are performed to obtain a better understanding of the relation between the microscopic structure, molecular interactions, and thermophysical properties of aqueous reline and ethaline solutions at temperatures ranging from 303.15 to 363.15 K. For both reline and ethaline solutions, the hydrogen bond (HB) networks disappear with increasing mass fraction of water, and the intensity of radial distribution function (RDF) peaks decreases. For a mass fraction of water of 40%, most of the HBs between the compounds of reline and ethaline are broken, and DESs are fully dissolved in water. Consequently, a monotonic decrease in viscosities and an increase in self-diffusion coefficients are observed. Ionic conductivities show a nonmonotonic behavior with increasing water content. Up to 60% water mass fraction, the ionic conductivities increase with increasing water content. A further increase in the mass fraction of water decreases conductivities. For all studied systems, the HB network and the peaks of RDFs show relatively small changes for water mass fractions below 5% and beyond 40%. The MD results show that viscosities decrease with temperature, while diffusivities and ionic conductivities increase. The effect of the temperature on the structure of DES−water mixtures is negligible.

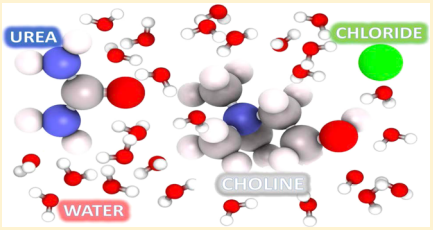

1. INTRODUCTION

Developing cost-effective, environmentally friendly, and sustainable solvents is a major challenge for the chemical industry.[1−3] Possible green alternatives to the conventional organic solvents (i.e., toluene, xylene, and benzene), which exhibit high toxicity and volatility, are urgently needed.[4] In this regard, ionic liquids (ILs) gained much interest. ILs exhibit interesting properties such as low vapor pressures, high thermal stability, low melting points (i.e., large liquid range), a large electrochemical window, high solubility, and nonflammability.[5−9]

Recently, deep eutectic solvents (DESs) are recognized as very promising solvents, sharing similar physicochemical properties with ILs. DESs are environmentally friendly solvents because they are often nontoxic, highly biodegradable, and biocompatible.[9−12] DESs are formed by a quaternary salt and a hydrogen bond donor (HBD) in a specific mixing ratio.[12] The term "eutectic" refers to the final compound, which has a much lower melting point than the one of each individual component or of the mixture at any other composition.[12] Low-cost materials and easy synthesis also make DESs cost-effective for large-scale production. DESs are used in a wide array of applications spanning metal coatings,[13,14] nanoparticle synthesis,[15,16] water decontamination,[17,18] biomass treatment,[19] and gas sequestration.[20]

Choline chloride-based (ChCl-based) DESs are one of the most well-known and well-studied types of DESs. ChCl is an inexpensive, nontoxic, and biodegradable ammonium salt that can form various DESs when combined with carboxylic acids, amides, or polyols such as malonic acid, urea, glycerol, and ethylene glycol (EG).[9] This diversity allows for many potential applications. For example, a ChCl/urea eutectic mixture (reline) is used for electrodeposition of metals to prepare semiconductors in thin-film solar cells.[21] ChCl/EG (ethaline) is used in electroplating and electropolishing.[22] ChCl/glycerol (glyceline) is an efficient medium for extraction of glycerol from biodiesel.[23] Glyceline is also a strong lubricant, particularly useful in marine industry.[24] ChCl/malonic acid (maline) DES is used for the synthesis of open-framework metal structures for catalysis applications.[25]

For the optimum design and characterization of green solvents based on DESs for industrial applications, it is crucial that control over the thermophysical properties is established. A proposed way to obtain such control is by adding small amounts of water into DES.[26,27] This is a simple, cheap, and clean way for creating solvents with modified properties because the presence of water alters the molecular structure of

Received: October 16, 2019
Revised: December 1, 2019
Published: December 3, 2019

DOI: 10.1021/acs.jpcb.9b09729
J. Phys. Chem. B 2019, 123, 11014−11025

DESs [i.e., hydrogen bond (HB) networks]. The addition of water affects the overall macroscopic properties of the fluid. Experimental studies have shown that the densities and viscosities of DES solutions (i.e., reline, glyceline, and ethaline) decrease with increasing water content as well as increasing temperature.[26,28,29] Leron and Li[30,31] investigated how pressure affects the volumetric properties of aqueous solutions of reline and ethaline for pressures up to 50 MPa at various temperatures. Shekaari et al.[32] measured the densities, speed of sound, viscosities, and refractive indices of aqueous reline solutions and used these data to calculate other properties including excess molar volumes, thermal expansions, and isentropic compressibilities. It is also important to note that empirical models can alternatively provide a theoretical standpoint for describing the transport properties of the aqueous DES solutions. For example, Grunberg−Nissan, Fang-He, and Eyring-NTRL/MTSM models are used to predict the viscosities of liquid mixtures.[33−36] These empirical models are particularly useful for identifying the nonidealities in the viscosity of the mixture. Mjalli and Mousa compared the performance of different empirical models in predicting the viscosity of aqueous ChCl-based DESs.[35] The Fang-He model is able to sufficiently predict the viscosities of size-asymmetric mixtures containing large and small molecules such as aqueous mixtures of ILs/DESs.[36]

Although experimental measurements are the main source of information on the macroscopic behavior of aqueous solutions of DESs, the resolution of experiments is typically too large for exploring changes at the molecular level. Thus, not much insight into the underlying physicochemical mechanisms can be provided by experiments alone. Molecular simulations are a powerful tool that can be used to explain and complement experiments. Perkins et al.[37] performed molecular dynamics (MD) simulations to predict several thermodynamic and transport properties of neat ChCl-based DESs and compared simulation results with available experimental findings. By analyzing the HB network and the radial distribution functions (RDFs), the microstructure of DESs was correlated to data measured with infrared spectroscopy.[38] Shah and Mjalli[27] carried out MD simulations to investigate the intermolecular structure of aqueous mixtures of reline. In the same study, experiments were also performed to measure several physical−chemical properties (i.e., densities, speed of sound, viscosities, melting points, conductivities, and so forth) as a function of the mole fraction of water at room temperature.[27] Recently, the influence of the hydration of different DESs was investigated using MD simulations, particularly focusing on static properties including densities, RDFs, spatial distributions, and hydrogen bonding.[39−41] Baz et al.[42] performed MD simulations to compute static and dynamic properties of glyceline−water mixtures at various temperatures. The simulations were additionally supported by equation-of-state modeling.

Environmentally benign and sustainable DESs have become an intriguing media for many applications. The strong influence of water on the structural, thermodynamic, and transport properties make water mixtures of DESs even more interesting. Contrary to the importance of DESs−water mixtures, only a very limited number of molecular simulation studies exist in literature, and thus, an enhanced understanding at the molecular level is still lacking. In this study, the main objective is to obtain insights into the relation between molecular interactions, microscopic structural heterogeneities, and thermophysical properties of ChCl-based DESs water mixtures. To this purpose, atomistic MD simulations of reline and ethaline aqueous solutions in the temperature range 303.15−363.15 K were performed. This study provides a detailed description on the structural, volumetric, and transport properties of aqueous mixtures of DESs. We systematically present variations in density, thermal expansivity, viscosity, self-diffusivity, ionic conductivity, RDFs, and HB distributions as a function of the water content and temperature. It is shown that the increase of the water content in the mixture results in a significant decrease in densities and viscosities of aqueous reline and ethaline solutions, while self-diffusivities are increased. For both water−reline and water−ethaline mixtures, ionic conductivities exhibit a non-monotonic behavior with increasing water content. These changes in the transport properties are found to be closely related to the HB network and RDFs. The rest of this paper is organized as follows: in Section 2, the details of the molecular models and methods used in this study are discussed. The results are presented in Section 3. The main conclusions are presented in Section 4.

2. MODELS AND METHODS

2.1. Force Fields. In the present study, the generalized amber force field (GAFF) was used to model aqueous reline and ethaline solutions.[43] The partial charges of each component were obtained using restrained electrostatic potential charge derivations.[38] The electrostatic potential was determined using the HF/6.31G* level of theory. Because electrostatic interactions are typically overpredicted when simulating ILs or DESs, a reduced-charge model is used.[27,37] The partial charges of ChCl in reline were scaled by a constant factor of 0.8. The partial charges of ChCl in ethaline were scaled by 0.9. These scaling constants were based on the earlier work by Perkins et al.,[37,38] in which the simulated densities and transport properties of neat reline and ethaline solutions using GAFF and reduced charges showed an excellent agreement with experimental results. Recently, Baz et al.[42] showed that GAFF with modified charges can be used for the simulation of aqueous solutions of glyceline.[42] In the present study, the results are supported by the available experimental data for force field validation. In literature, several other force fields such as the OPLS−AA framework[44] and Merck Molecular force field[27] have been used to model DESs.

For the representation of water molecules, a rigid three-site SPC/E model was used. SPC/E can adequately reproduce transport properties of liquid water at various temperatures,[45,46] and it has been extensively used in simulations of aqueous electrolyte solutions and mixtures with ILs.[27,47,48] It is important to note here that the scope of this study is not to perform an exhaustive investigation of the accuracy of various force fields combinations but to provide physical insights into the structural and transport behavior of DES−water mixtures. All force field parameters are listed in Tables S1−S11 of the Supporting Information.

2.2. Simulation Details. In all our MD simulations, periodic boundary conditions were applied in all directions. To achieve eutectic compositions at a 1:2 molar ratio, each reline solution consisted of 50 ChCl and 100 urea molecules. Each ethaline solution consisted of 50 ChCl and 100 EG molecules. The number of water molecules was determined based on the desired water content. The mass fraction of water (ω_w) can be calculated from

DOI: 10.1021/acs.jpcb.9b09729
J. Phys. Chem. B 2019, 123, 11014−11025

$$\omega_w = \frac{N_w M_w}{N_{ChCl} M_{ChCl} + N_{HBD} M_{HBD} + N_w M_w} \quad (1)$$

where M_i and N_i are the molecular weight and the number of molecules of species i, respectively. The mass fraction of DES (ω_{DES}) is $\omega_{DES} = 1 - \omega_w$. In Table S12 of the Supporting Information, all simulated mixtures in the present study are listed.

Initial configurations were randomly generated in a cubic simulation box with an initial length of 10 nm using the Packmol software.[49] All simulations were carried out using the large-scale atomic/molecular massively parallel simulator (LAMMPS), version released on August, 2018.[50] Long-range electrostatic interactions between charged species were handled using the particle−particle, particle-mesh (pppm) method with a root-mean accuracy of 10^{-6}.[51] Short-range interactions were smoothly truncated at a cutoff distance of 1.3 nm. The Lorentz−Berthelot combining rules were used for the interactions between dissimilar atoms.[52] Bond lengths and bond-bending angles of water molecules were kept rigid using the SHAKE algorithm in LAMMPS.[53] To integrate Newton's equations of motion, the Verlet algorithm was used with a time step of 1 fs.

In this study, five different temperatures in the range of 303.15−363.15 K were considered at 1 atm. All properties were computed in the following way: initially, energy minimization was performed using the conjugate gradient method for 10 000 steps. Then, MD runs in the isothermal−isobaric (*NPT*) ensemble were performed to compute average volumes and densities for 12 ns using a time step of 1 fs. The average box lengths for all simulated mixtures for the whole temperature range are listed in Table S13 of the Supporting Information. Consecutively, starting from the average volumes computed from the *NPT* simulations, each system was allowed to equilibrate for 1 ns at the desired temperature in the canonical (*NVT*) ensemble. After the equilibration, all transport properties were computed from production runs in the microcanonical (*NVE*) ensemble. The simulation lengths varied from 30 to 100 ns, based on the system. The longer sampling times are required because of the slow dynamics of DESs mixtures with low water contents.[38] This simulation procedure (i.e., *NPT* to *NVT* to *NVE*) is also explained in detail in the Supporting Information document in a recent study by Jamali et al.[54] All transport properties were computed using the OCTP (on-the-fly computation of transport properties) plugin in LAMMPS.[54] OCTP uses the Einstein relations combined with the order-*n* algorithm.[55,56] Details on the inner workings of the OCTP plugin can be found in the study by Jamali et al.[54] All RDFs were also calculated using the OCTP tool. The RDFs reported in the present study were corrected for finite-size effect based on the work by van der Vegt and co-workers.[57−59] HB analysis was performed using the HBonds plugin in VMD (visual MDs).[60] Uncertainties for all properties were calculated based on the standard deviation from six independent simulations, each one started from a different initial configuration.

3. RESULTS AND DISCUSSION

The volumetric and transport properties of reline and ethaline solutions are discussed in Sections 3.1 and 3.2. In Section 3.3, a thorough discussion on how the structure of the fluid, expressed by the computed RDFs and HBs, can be related to the variations in the volumetric and transport properties of the DESs−water mixtures is presented. All raw data are listed in Tables S13−S23 of the Supporting Information.

3.1. Volumetric Properties. The computed densities of aqueous reline and ethaline solutions as a function of temperature and mass fraction of water are presented in Figure 1. All mixtures are in good agreement with the

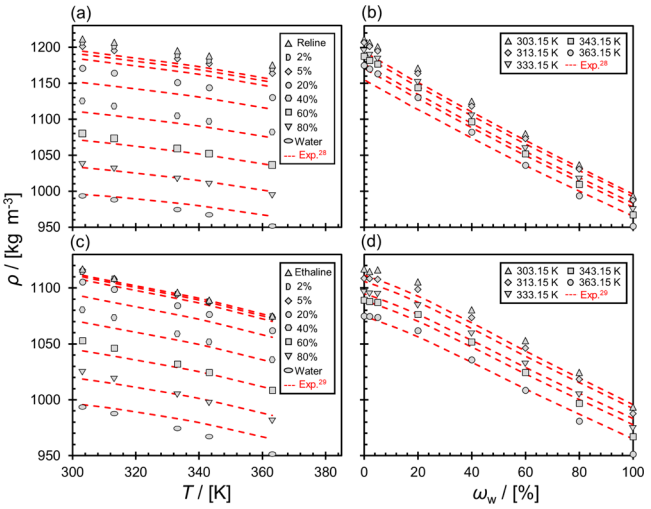

Figure 1. Densities of aqueous reline solutions as a function of (a) temperature and (b) mass fraction of water. Densities of aqueous ethaline solutions as a function of (c) temperature and (d) mass fraction of water. Gray symbols represent the MD results. Red dashed lines refer to experimental data taken from earlier work.[28,29]

experimental values by Yadav et al.,[28,29] showing deviations up to 1.7%. The numerical values of the computed densities are listed in Tables S14 and S15 of the Supporting Information. In most reline and ethaline solutions, MD simulations slightly overpredict the experimental densities. This overprediction can be attributed to the slightly increased attractive forces between water and the components of the DESs, imposed by the force fields used. Similar findings were also presented for glyceline−water mixtures in an earlier study by Baz and co-workers.[42] As shown in Figures 1b,d, the densities for both reline and ethaline solutions gradually decrease with increasing water content. An addition of 2 and 5% water to the pure component shows a marginal decrease on the density. The densities of ethaline solutions are lower compared to those of reline. This is mainly because urea is denser than EG. The computed densities decrease with increasing temperature, which is typical for aqueous solutions. For temperatures ranging from 303.15 to 363.15 K, the density of neat reline is between 1211.3 and 1175.4 kg/m^3, while density of neat ethaline is between 1116.9 and 1074.8 kg/m^3. These values are in excellent agreement with other MD and experimental results of neat reline[27,28,30,38,61] and ethaline[29,31,37,61] solutions.

The temperature dependence of density is typically quantified by the volumetric thermal expansion coefficient (α_p) of the liquid[62]

$$\alpha_p = \frac{1}{\rho}\left(\frac{\partial \rho}{\partial T}\right)_p \quad (2)$$

where ρ is the density and T is the temperature. $(\partial\rho/\partial T)_p$ can be calculated from the slope of the density−temperature curves in Figures 1a,c. The computed thermal expansion coefficients as a function of the water content are presented in Tables S16

DOI: 10.1021/acs.jpcb.9b09729
J. Phys. Chem. B 2019, 123, 11014−11025

and S17 in the Supporting Information. Experiments and MD predictions show deviations up to 25%. These deviations can be mainly attributed to the performance of the force fields for various temperatures. This was also pointed out in the study by Baz et al.[42] More accurate α_p can be possibly computed after an elaborate refinement of the force field and the partial charges.

3.2. Transport Properties. *3.2.1. Viscosity.* In Figure 2, the computed viscosities of aqueous reline and ethaline

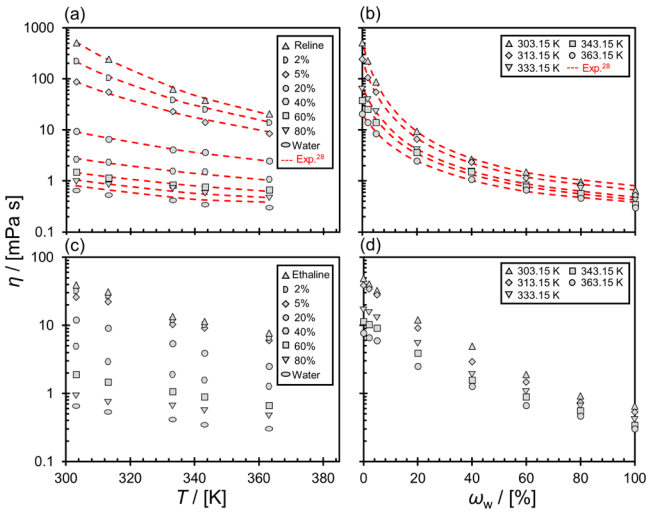

Figure 2. Viscosities of aqueous reline solutions as a function of (a) temperature and (b) mass fraction of water. Viscosities of aqueous ethaline solutions as a function of (c) temperature and (d) mass fraction of water. Gray symbols represent the MD results. Red dashed lines refer to experimental data taken from earlier work.[28] The statistical uncertainties can be found in Tables S18 and S19 of the Supporting Information.

solutions as a function of temperature and mass fraction of water are shown. The MD results for reline solutions are compared with the available experimental data measured by Yadav and Pandey using a rolling-ball microviscometer.[28] The deviations between experimental and computed viscosities of reline/water mixtures are less than 14% in all cases. For pure water, MD results with the SPC/E water model deviate approximately 20% from experiments. This was also shown in other studies.[63,64] All computed viscosities, along with the available experimental values, are listed in Tables S18 and S19 of the Supporting Information. For neat ethaline solutions, simulations and experiments are in reasonable agreement at all temperatures as shown in Figure S3 of the Supporting Information. As shown in Figures 2b,d, the viscosities of all reline−water and ethaline−water mixtures monotonically decrease with increasing water content. Reline is more viscous than ethaline. The viscosities of neat reline and ethaline at 303.15 K are approximately 511 and 39 MPa·s, respectively. The MD simulations showed that the addition of a small amount of water (i.e., 2%) significantly reduces the viscosities to 226 and 32 MPa·s, respectively. A further increase of mass fraction of water to 5% causes approximately 83 and 30% reduction in the viscosity of neat reline and ethaline, respectively. Viscosities also decrease with increasing temperature. Increasing temperature from 303.15 to 363.15 K results in 25 times reduction in the viscosity of neat reline. For the same temperature range, the reduction is five times for neat ethaline. As the mass fraction of water increases, the strong temperature dependency of viscosity disappears. The viscosity of the reline mixture with 80% mass fraction of water decreases by a factor of 2 as temperature increases from 303.15 to 363.15 K. The viscosity of neat ethaline decreases by a factor of 5 in the same temperature range, while the viscosity of the ethaline−80% water mixture decreases 2 times. These findings are consistent with trends obtained in earlier studies.[26,28,42]

3.2.2. Self-Diffusivity. The self-diffusion coefficients in the present study are corrected for finite-size effects using the Yeh−Hummer correction[65,66]

$$D_\infty = D_{MD} + \frac{k_B T \xi}{6\pi\eta L} \tag{3}$$

where D_∞ is the corrected self-diffusion coefficient (thermodynamic limit), D_{MD} is the size-dependent self-diffusion coefficient computed in MD simulations, k_B is the Boltzmann constant, L is the length of the simulation box, T is the temperature, η is the shear viscosity computed in MD, and ξ = 2.837298 is a dimensionless constant.

In Figure 3, the computed self-diffusion coefficients of the HBD (urea), cation (Ch^+), and anion (Cl^-) in reline solutions

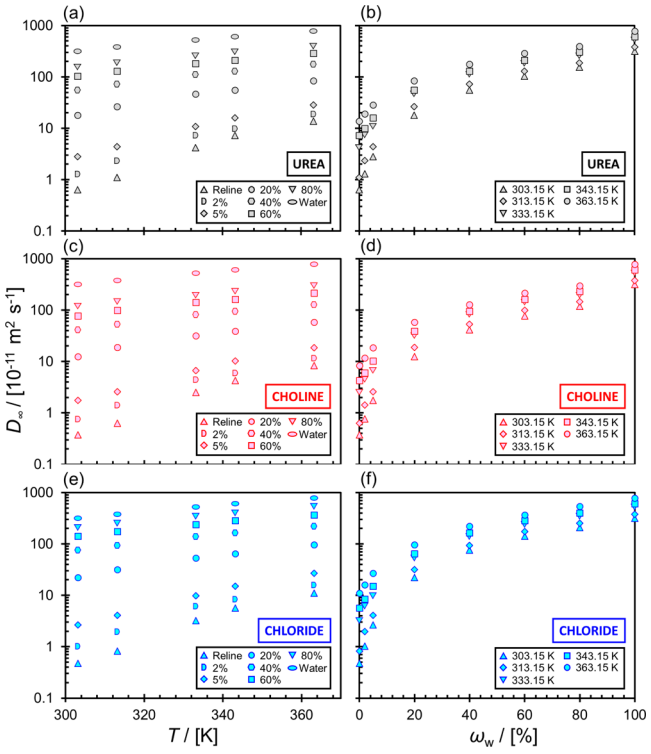

Figure 3. Self-diffusion coefficients corrected for finite-size effects in reline−water mixtures: for urea as a function of (a) temperature and (b) mass fraction of water, for the choline cation as a function of (c) temperature and (d) mass fraction of water, and for the chloride anion as a function of (e) temperature and (f) mass fraction of water. The statistical uncertainties can be found in Table S20 of the Supporting Information.

are shown as a function of temperature and mass fraction of water. The self-diffusion coefficient of each component monotonically increases with increasing water content, as well as increasing temperature. As can be seen in Figure 3, the diffusivity of Cl^- is mostly affected by the change in the mass fraction of water. At 303.15 K, the self-diffusion coefficient of

DOI: 10.1021/acs.jpcb.9b09729
J. Phys. Chem. B 2019, 123, 11014−11025

Cl^- exhibits an increase of approximately 439 times when the mass fraction of water increases from 0 to 80%. For Ch^+ and urea, the corresponding increase is 319 and 243 times, respectively. At higher temperatures, the respective increase in the self-diffusion coefficients of the anion, cation, and HBD is almost the same. Considering a reline solution with 5% mass fraction of water, the self-diffusivities of urea, Ch^+ and Cl^- increase approximately by a factor of 10 when temperature is increased from 303.15 to 363.15 K. Such an increase in temperature results in 10 times reduction in the viscosity of the respective system. The temperature dependency of self-diffusivity becomes less pronounced as the water content increases. This is expected due to the lower density of water compared to the DES. For the neat reline, a temperature increase from 303.15 to 363.15 K leads to approximately 22 times increase in the self-diffusion coefficient. The respective increase for the mixture of reline with 80% water is only 2.5 times. The self-diffusion coefficient of urea is always higher than that of Ch^+, independent of the water content. The main reason for this behavior is that the molecular mass of the Ch^+ cation (104.2 g/mol) is almost twice the mass of urea (60.1 g/mol). However, this is not the case for the self-diffusivity of Cl^-. In a neat reline solution, urea diffuses faster than Cl^- ions (35.5 g/mol), although it is heavier. Perkins et al.[38] suggested that this behavior is due to the strong HBs between urea−urea and urea−anion, resulting in larger mobility in urea than Cl^-. The addition of water eradicates the strong hydrogen bonding between urea−Cl^- and urea−urea. In aqueous reline solutions with more than 20% water mass fraction, urea molecules diffuse slower than Cl^- ions as a result of the strong depletion of HBs. It is important to note that in addition to the molecular weight, the hydrodynamic radius is another important factor that drastically affects the self-diffusivity of ions. Thus, the kinetic behavior of the ions is determined by the interplay between molecular weight and radius and the structure of the fluid.

The self-diffusion coefficients of the HBD (EG), cation (Ch^+), and anion (Cl^-) in ethaline solutions are shown in Figure 4. As can be seen, all self-diffusion coefficients increase with the water content. This increase for ethaline mixtures is less prominent when compared to the respective reline solutions. Considering the self-diffusivity of Cl^- at 303.15 K, an increase of 43 times is observed when 80% of water is added to the neat ethaline. The respective increase in reline solution is 439 times. The largest increase in diffusion coefficients for ethaline with increasing water content is for Cl^-, followed by Ch^+ and HBD. This is strongly related to the disappearance of HBs between the various species of DESs as explained earlier. All self-diffusion coefficients of ethaline mixtures increase as temperature increases. At small mass fractions of water, the temperature dependency of self-diffusion coefficients of ethaline is less prominent when compared to that of reline. At big mass fractions of water, the temperature effect on reline and ethaline solutions is similar. For aqueous reline and ethaline solutions with 80% water content, an increase in temperature from 303.15 to 363.15 K results in 2.5 and 2.6 times increase in the self-diffusivities of Cl^- ions, respectively. The self-diffusion coefficient of EG is always higher than that of Ch^+, mainly due to the lower molecular weight of EG (62.1 g/mol). This behavior is independent of the mass fraction of water. Despite the fact that EG is heavier than Cl^-, the self-diffusion coefficient of EG is higher due to the presence of strong HBs between the anion and HBD, as discussed earlier.

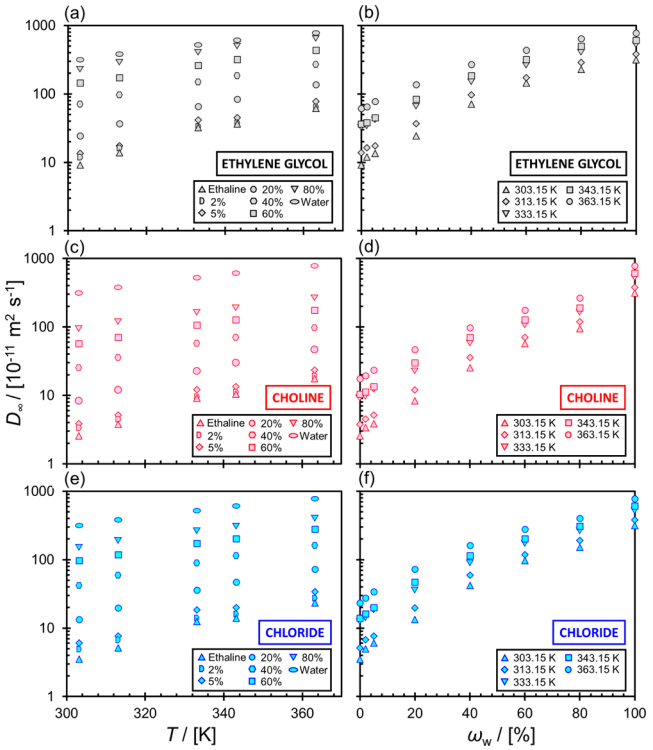

Figure 4. Self-diffusion coefficients corrected for finite-size effects in ethaline−water mixtures: for ethylene glycol as a function of (a) temperature and (b) mass fraction of water, for the choline cation as a function of (c) temperature and (d) mass fraction of water, and for the chloride anion as a function of (e) temperature and (f) mass fraction of water. The statistical uncertainties can be found in Table S21 of the Supporting Information.

In Figure S4 of the Supporting Information, the MD results of neat reline and ethaline are compared with experimental data by D'Agostino et al.[67] The computed self-diffusion coefficients of neat reline and ethaline show deviations of up to 35% compared with earlier MD and experimental studies.[37,38,67] In an experimental study by D'Agostino et al.,[68] self-diffusivities and viscosities of aqueous reline and ethaline solutions at low mass fractions of water (i.e., up to 17.5%) at 293.15 K are reported. Results at this lower temperature indicate similar trends with our predictions of viscosities and self-diffusivities using MD simulations. The computed self-diffusion coefficients of pure water are in close agreement with experiments for the entire temperature range studied.[69] All results related to the self-diffusion coefficients are listed in Tables S20 and S21 of the Supporting Information.

3.2.3. Ionic Conductivity. The ionic conductivity can be directly associated with the degree of fluidity (reciprocal of viscosity) in a liquid. High viscosity indicates low molecular mobility, which leads to low conductivity of the liquid.[70] To compute the ionic conductivity (κ) of DES−water mixtures, the Nernst−Einstein (NE) equation is used[71]

$$\kappa = \frac{e^2}{k_B TV} \sum_i N_i q_i^{\,2} D_i \tag{4}$$

where N_i is the number of molecules of type i, q_i is the charge of molecules of type i, D_i is the computed self-diffusion coefficient of molecules of type i, and e is the elementary charge. In the case of aqueous reline and ethaline solutions, the Nernst−Einstein equation includes only anions and cations

DOI: 10.1021/acs.jpcb.9b09729
J. Phys. Chem. B 2019, 123, 11014−11025

because HBDs and water molecules are charge-neutral. The computed ionic conductivities of reline and ethaline solutions are shown in Figure 5. For both DESs solutions, the ionic

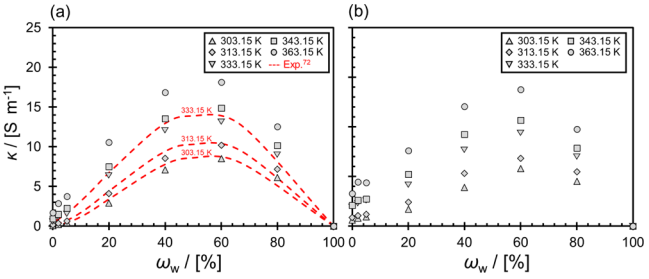

Figure 5. Ionic conductivities of (a) reline–water mixtures and (b) ethaline–water mixtures as a function of mass fraction of water. Gray symbols represent the computed ionic conductivities at various temperatures. The red dashed lines refer to experimental data taken from an earlier work.[72]

conductivities show a nonmonotonic behavior with increasing water content. Neat DESs have low conductivities, mainly due to the low ionic mobilities. The ionic conductivities increase with the addition of water. This is mainly related to the increased mobility due to the disappearing HBs between HBDs–anions and anions–cations. As can be seen from Figures 5a,b, conductivities reach a maximum at approximately 60% water mass fraction. Beyond this, water–water interactions become dominant, and thus, conductivity gradually decreases. For both reline and ethaline solutions, ionic conductivities increase with increasing temperatures. This is again due to the enhancement of ionic mobility as temperature increases. The computed ionic conductivity of ethaline solution is higher than that of reline at low mass fractions of water (<20%). The opposite is evident for mass fractions of water above 20%.

In Figure 5a, the experimental and simulated ionic conductivities of reline solutions at three different temperatures, that is, 303.15, 313.15, and 333.15 K, are compared. The experimental data were taken from a recent study by Agieienko and Buchner.[72] The MD simulations are in close agreement with the experiments. This is a strong indication that the computed self-diffusion coefficients (Figure 4) are accurate. To the best of our knowledge, no experimental results on the ionic conductivity of ethaline–water mixtures are available; thus, no comparison with the MD data shown in Figure 5b can be done. In Figure S5 of the Supporting Information, the computed conductivities of neat ethaline and reline at various temperatures are compared with experimental results. For neat ethaline, the ionic conductivities obtained from MD simulations are in line with the experimental results by Mjalli and Ahmed.[73] All raw data on ionic conductivities of aqueous reline and ethaline solutions are listed in Tables S22 and S23 of the Supporting Information, respectively. In this study, the ionic conductivities of DES–water mixtures are computed from the NE equation using the self-diffusivities obtained from MD simulations. This is an indirect method to compute ionic conductivities. Alternatively, ionic conductivities can be computed by the autocorrelation of charge current.[74] In the works by Tu et al.[74] and Humbert et al.,[71] a discussion about the accuracy of two methods is presented.

3.3. Structure. *3.3.1. Radial Distribution Functions.* The RDFs for various components of aqueous reline solution for the entire range of mass fractions of water at 303.15 K are shown in Figure 6. With the addition of water, the intensity of the first RDF peaks between urea–Cl^- and Ch^+–Cl^- decreases, as shown in Figures 6a,e, respectively. This indicates that the interactions between these molecules become weaker. The first RDF peaks of urea–Ch^+ and urea–urea increase with the addition of water as shown in Figures 6b,c, respectively. It is important to note that the intensity of the first RDF peaks between urea–Cl^- and Ch^+–Cl^- is more pronounced when compared to those of urea–urea and urea–Ch^+ sites. Therefore, the former is more effective on the physical characteristic of the reline–water mixture. The positions of the peaks for urea–Cl^-, Ch^+–Cl^-, and urea–Ch^+ do not significantly change with the addition of water. The first peaks are approximately placed at a distance of 4.2 Å for urea–Cl^-, 4.5 Å for Ch^+–Cl^-, and 4.7 Å for urea–Ch^+. These are in agreement with RDFs based on neutron diffraction (ND)

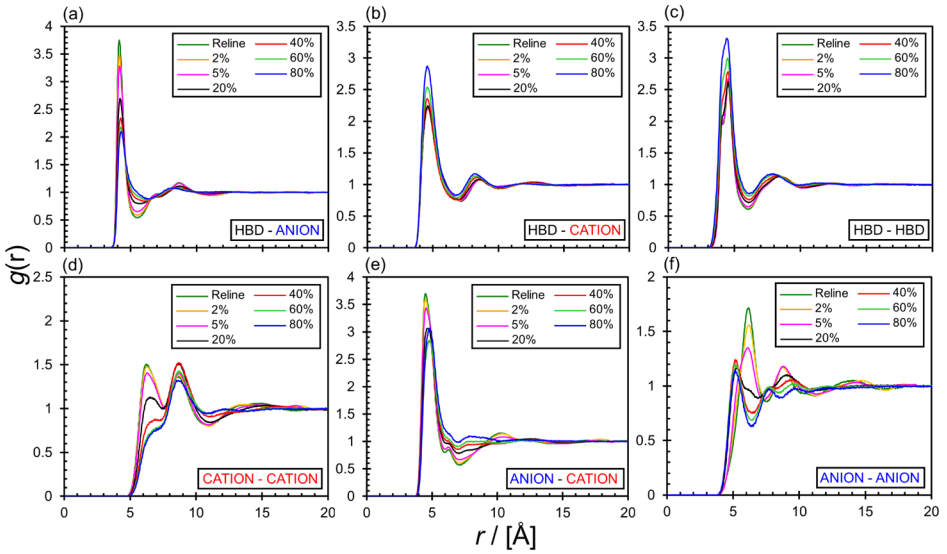

Figure 6. RDFs of (a) urea–Cl^-, (b) urea–Ch^+, (c) urea–urea, (d) Ch^+–Ch^+, (e) Cl^-–Ch^+, and (f) Cl^-–Cl^- in aqueous reline solution as a function of the mass fraction of water at 303.15 K.

DOI: 10.1021/acs.jpcb.9b09729
J. Phys. Chem. B 2019, 123, 11014–11025

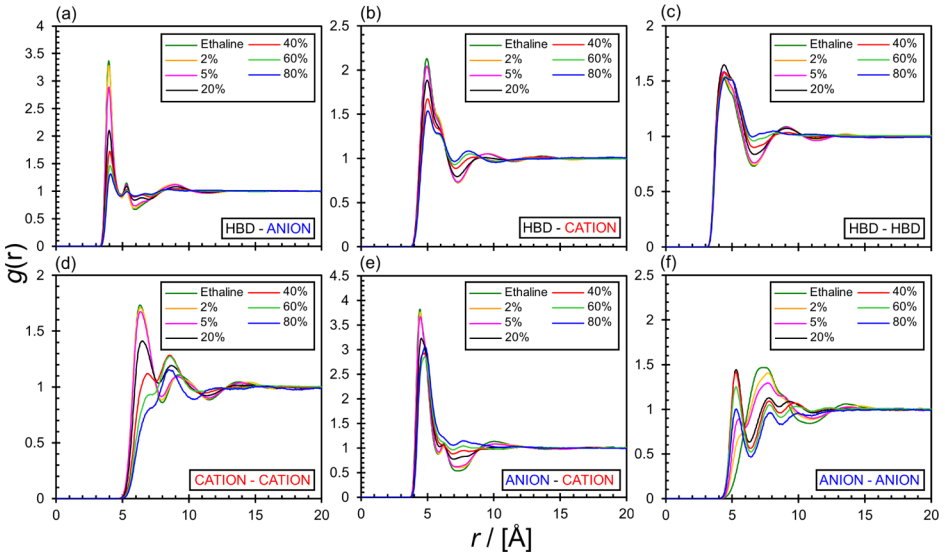

Figure 7. RDFs of (a) ethylene glycol−Cl^-, (b) ethylene glycol−Ch^+, (c) ethylene glycol−ethylene glycol, (d) Ch^+−Ch^+, (e) Cl^-−Ch^+, and (f) Cl^-−Cl^- in aqueous ethaline solution as a function of the mass fraction of water at 303.15 K.

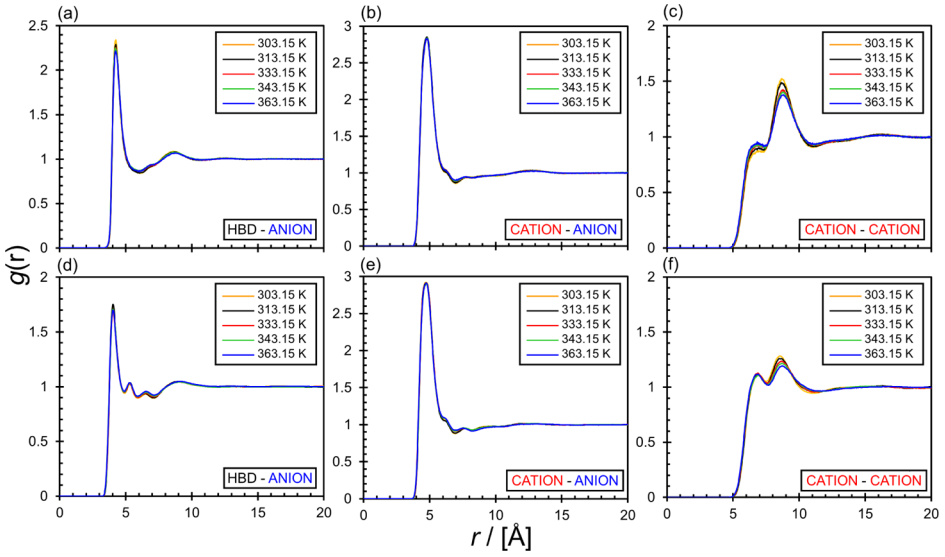

Figure 8. RDFs as a function of temperature of (a) urea−Cl^-, (b) Ch^+−Cl^-, and (c) Ch^+−Ch^+ in the reline−water mixture with a mass fraction of water of 40%. RDFs as a function of the temperature for (d) ethylene glycol−Ch^+, (e) Ch^+−Cl^-, and (f) Ch^+−Ch^+ in the ethaline−water mixture with a mass fraction of water of 40%.

experiments of reline, in which RDFs were obtained using the Empirical Potential Structure Refinement model fitted to the experimental data.[75] The cation−cation RDF peaks are located at a larger distance compared to those of other components. The main reason for this behavior is most probably the size and the structural asymmetry of choline. The RDF peaks of Ch^+−Ch^+ and Cl^-−Cl^- also show a gradual decrease with increasing water content as shown in Figures 6d,f. For these pairs, the locations of the peaks vary with the mass fraction of water. Beyond 20%, the peak of the first solvation shell for the Ch^+−Ch^+ pair almost vanishes, and another peak is formed at a larger distance as shown in Figure 6d. This indicates that Ch^+ ions tend to move away from each other in the presence of water, and water molecules gradually permeate between Ch^+ ions. As for Cl^-−Cl^-, less pronounced peaks at shorter distances are formed for mass fractions of water larger than 20% as shown in Figure 6d. Cl^- ions come closer to each other with increasing mass fraction of water. This indicates that water prefers to be closer to the anions rather than cations.[27,40,41]

The RDFs of ethaline−water mixtures at 303.15 K are presented in Figure 7. The intensity of the first RDF peak for all pairs decreases with increasing water content, indicating that the intermolecular interactions of ethaline become weaker in the presence of water. A strong decrease is obtained for EG−Cl^-, EG−Ch^+, and Ch^+−Cl^- interactions with the increased water content, as shown in Figures 7a,b,e, respectively. Subtle variations exist for EG−EG with increasing water content as shown in Figure 7c. It is important to note that these variations become more pronounced for 20% water mass fractions and above. The locations of the first peaks are 4.0 Å for EG−Cl^-, 4.5 Å for Ch^+−Cl^-, and 5.0 Å for EG−Ch^+. The peak locations remain almost the same with increasing water content for all molecular pairs, except for Ch^+−Ch^+ and

DOI: 10.1021/acs.jpcb.9b09729
J. Phys. Chem. B 2019, 123, 11014−11025

Cl^-−Cl^- as shown in Figures 7d,f, respectively. With increasing water content, new RDF peaks of Cl^-−Cl^- are formed at a shorter distance. Ch^+−Ch^+ peaks are formed at higher distances with increasing water content. In addition, peaks of EG−Cl^- are more intense, and slightly closer to each other, than peaks of EG−Ch^+, indicating that EG prefers to be closer to the anions.

All water-related RDFs for reline and ethaline are shown in Figures S6 and S7 of the Supporting Information, respectively. For both reline and ethaline solutions, peaks are sharper for Cl^-−water compared to those of Ch^+−water and HBD−water. The locations of the first peaks do not significantly change with increasing water content. The first peaks are placed approximately at 3.3 Å distance for Cl^-−water, 3.7 Å distance for urea−water, and 4.4 Å distance for Ch^+−water for reline. For ethaline cases, the first peaks are located at approximately 3.2 Å distance for Cl^-−water, 3.5 Å distance for EG−water, and 4.4 Å distance for Ch^+−water for ethaline. These indicate that water molecules are in a closer proximity to the anions than cations and HBD, in both reline and ethaline solutions. RDFs between Cl^-−water and Ch^+−water slightly shift to the left with increasing water content. Gao et al.[76] reported that this is mainly due to the shrinking hydration shell of Cl^- as the water content increases. Also, cation−water RDFs span a wider distribution than those of the water−anion and water−cation. This is mainly because of the larger size and asymmetry of the choline cation.[41,76] The peaks for all pairs decrease with increasing water content. The most prominent reduction is observed for anion−water interactions. This clearly indicates the critical role of the anion on the physical properties of DES solution.

The effect of temperature on the structure in DES−water mixtures is shown in Figure 8. The RDFs between HBD−anion, cation−anion, and cation−cation of aqueous reline and ethaline mixtures are shown only for 40% water mass fraction for brevity. The RDFs for all other components of DESs can be found in Figures S8 and S9 of the Supporting Information. Our results indicate that the temperature has a minor effect on RDFs in both reline and ethaline mixtures. This finding is in agreement with earlier studies.[40] The temperature-independent behavior is observed for the entire range of water composition. The only noticeable effect of temperature exists for the cases of the cation−cation and anion−anion. The intensity of the RDF peaks between these ions shows a slight decrease. As shown in an earlier study by D'Agostino et al.,[68] the addition of water in ethaline solutions allows for the exchange of ions, for example, OH proton on Ch^+. This results in mildly acidic solutions for ethaline. On the contrary, water leads to the formation of ammonium hydroxide in the case of reline, which is a basic solution.[68] As our simulations were performed with non-reactive force fields, such formations cannot be captured.

3.3.2. HB Distribution. As HB formation criteria, a cut-off distance of 3.5 Å for heavy-to-heavy atom and an angle of 30° between the donor−hydrogen−acceptor were used.[77,78] Figure 9a,b shows the total number of HBs in the aqueous reline and ethaline solutions at 303.15 K, respectively. In reline solutions, the presence of water leads to significant reduction on the HB population of urea−urea and urea−Cl^-. This reduction is less pronounced for urea−Ch^+ and Ch^+−Cl^-. At low water mass fractions (i.e., approx. 2%), the number of HBs between urea and any other molecule slightly increases, showing a deviation from the general trend. Shah and Mjalli[27] attribute this behavior to the enhanced interactions with the HB donor at

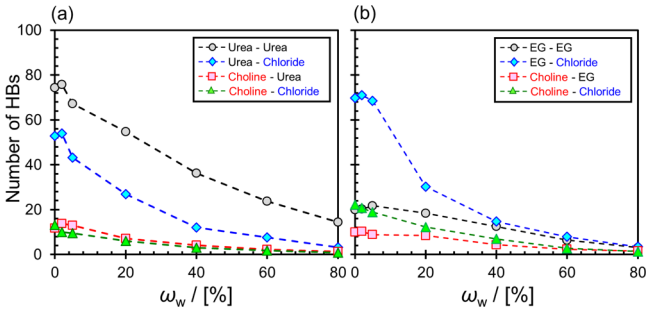

Figure 9. Number of hydrogen bonds as a function of the mass fraction of water (a) reline−water mixtures and (b) ethaline−water mixtures at 303.15 K. Each simulation of reline contains 50 choline chloride molecules and 100 urea molecules. Each simulation of ethaline simulation contains 50 choline chloride molecules and 100 ethylene glycol molecules.

this water content. With a further increase in the water content, a significant decrease in the number of HBs between urea−urea and urea−Cl^- is observed. Beyond water mass fractions of 40%, a relatively small decrease in the number of HBs between all possible pairs is obtained. Independent of the water content, the number of HBs in reline solutions order for Ch^+−Cl^-, Ch^+−urea, urea−Cl^-, and urea−urea, respectively. Note that the highest number of HBs is observed between urea−urea because the oxygen in urea is a stronger HB acceptor.[37] In the absence of water, urea makes approximately 0.8 HBs per urea with other urea molecules in the reline solutions. This goes down to 0.15 HBs per urea molecule for the reline−water mixture with 80% mass fraction of water. In addition, urea makes stronger HBs with the anion than the cation. For neat reline, there are 0.5 HBs per urea molecule for urea−Cl^-. There are 0.14 HBs per urea molecule for urea−Ch^+.

For ethaline−water mixtures, the number of HBs for all pairs exhibits a decreasing trend with increasing water content as shown in Figure 9b. The addition of water yields stronger influence on hydrogen bonding of EG−Cl^- when compared to EG−EG, Ch^+−EG, and Ch^+−Cl^-. Likewise to the results of reline, there is a slight increase in the number of HBs for EG−EG, Ch^+−EG, and Cl^-−EG at low mass fractions of water. For any ethaline−water mixture, the largest HB contribution is provided by EG−Cl^-. This is because the anion has the highest tendency to make HBs with water molecules compared to the other components of ethaline.[41] Our results further indicate that water preferentially solvates the Cl^- anion over cation.[41] This can be seen also by the HB networks between water molecules and the species of DESs, which are presented in Figure S10 of the Supporting Information. It is found that EG makes approximately 0.7 HBs per EG with the anions in the absence of water, whereas the addition of 80% of water greatly decreases this to 0.04 HBs per EG molecule. The HBs per EG for the EG−anion are almost seven times higher than the ones of the EG−cation for neat ethaline. This strong hydrogen bonding of the anion is the reason why it has the highest self-diffusion coefficient. Earlier MD simulations[27,40,41] and ND experiments[75,79] also pointed out that the Cl^- anion plays a central role on the microstructural arrangement mainly due to the strong intermolecular interactions and hydrogen bonding capability. In Figure S11 of the Supporting Information, the fractions of HBs for neat reline and ethaline are shown. For reline, the fractions of urea−urea, urea−Cl^-, Ch^+−Cl^-, and

DOI: 10.1021/acs.jpcb.9b09729
J. Phys. Chem. B 2019, 123, 11014−11025

Ch^+−urea are found to be 0.49, 0.35, 0.09, and 0.08, respectively. For ethaline, the fractions of EG−Cl^-, EG−EG Ch^+−Cl^-, and Ch^+−EG are found to be 0.57, 0.17, 0.16, and 0.08, respectively. These results are in close agreement with earlier MD results by Perkins et al.[37] (see Figure 9). In Figure 10, the effect of temperature on the hydrogen bonding

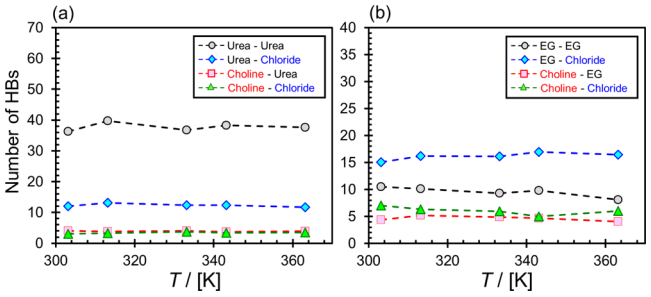

Figure 10. Number of hydrogen bonds as a function of temperature for the (a) reline−water mixture with a mass fraction of water of 40% and the (b) ethaline−water mixture with a mass fraction of water of 40%. Each simulation of reline contains 50 choline chloride molecules and 100 urea molecules. Each simulation of ethaline contains 50 choline chloride molecules and 100 ethylene glycol molecules.

behavior is presented. For brevity, results for only mass fraction of water of 40% are shown. For both reline and ethaline, temperature has negligible influence on the HB distribution. This finding is consistent with RDFs. In this study, the RDFs and HB networks are used to characterize the structure of reline and ethaline solutions. It is important to note here that other ways to characterize the structure of aqueous mixtures, such as coordination numbers,[80,81] spatial distribution functions,[40,44] and radial-angular distribution functions[40] can be also very useful. In Table S24 of the Supporting Information, the coordination numbers of reline and ethaline solutions are presented as a function of mass fraction of water. The coordination numbers are computed by integrating $g(r)$ to the first minimum of RDF.

The macroscopic properties of the reline and ethaline solutions are found to be closely related to the microscopic structure. The computed RDFs and HB distributions show that many strong changes occur in the microscopic structure for mass fractions of water between 5 and 40%. Strong depletion of the HBs and reduction in the intensity of the RDF peaks for the HBD−anion and anion−cation is observed. This indicates that the level of hydration of DESs is increased. As a result, fluidity increases, and thus, diffusivities and conductivities also increase. For mass fractions of water larger than 40%, the effect of water on the structure becomes less pronounced. Earlier simulation results by Shah and Mjalli[27] also showed that for mass fractions of water larger than 25%, the compounds of reline are fully hydrolyzed. Neutron scattering experiments by Hammond et al.[79] showed that reline loses its microscopic structure at approximately 42% mass fraction of water. As shown in Figure 9b, for ethaline solutions, the most HBs are formed by the HBD−anion pair. In the case of reline, both HBD−HBD and HBD−anion are dominant as shown in Figure 9a. This is mainly because urea is a stronger HB acceptor than EG. The strong hydrogen bonding character of urea, with other ureas and Cl^-, makes reline less viscous than ethaline. At high water contents (at which the solution becomes more dilute), the number of HBs diminish, and thus, similar viscosity values are observed for reline and ethaline. In this study, reasonable agreement with experimental data for various transport, thermodynamic, and structural properties of aqueous reline and ethaline mixtures were obtained by using combinations of fixed-point charged force fields. This does not guarantee that the predictive ability of these force fields will be as good for any property of aqueous DESs solutions and/or for any DES. For more information on the effect of polarizability on the structural, volumetric, and transport properties of aqueous ILs/DESs/ionic solutions, the reader is referred to the studies by Kelkar et al.,[82] Salanne et al.,[83] Jiang et al.,[84] and Hunt.[85]

4. CONCLUSIONS

MD simulations of aqueous reline and ethaline solutions were carried out to explain how the microscopic structure affects the thermodynamic and transport properties. The densities and viscosities of aqueous reline and ethaline solutions exhibit a monotonic decrease with increasing water content. As expected, the self-diffusivities show a monotonic increase. The viscosity of reline−water mixture is larger than the viscosity of the ethaline−water mixture. This is mainly due to the stronger hydrogen bonding character of urea compared to EG. Thus, reline is affected more by changes in the water content. With the addition of even small amounts of water (e.g., 2%) at 303.15 K, the viscosity of reline solution drops nearly to 50% of neat reline, and the viscosity of ethaline solution drops to 20% of neat ethaline. The self-diffusivities of anions exhibit a much more pronounced increase with increasing water content compared to the self-diffusivity of HBDs and cations for both reline and ethaline solutions. This behavior is related to the strong depletion of the HBs between anion and HBDs as the water mass fraction increases. Using the computed diffusivities, ionic conductivities are calculated by the NE relation. A nonmonotonic behavior is obtained with increasing water content with a maximum observed at 60%. At low mass fractions of water (i.e., <5%), the RDFs and hydrogen bonding network in reline and ethaline solutions slightly change. An increase in the mass fraction of water up to 40% significantly reduces the number of HBs between urea−anion and urea−urea in reline solution and the number of HBs between the EG and the anion for ethaline solution. For a mass fraction of water beyond 40% less influence on the RDFs and HBs can be observed. This indicates that reline and ethaline lose their intermolecular structure and dissolve in water. Consequently, viscosities decrease, and thus, self-diffusivities increase. The computed transport properties of aqueous DES solutions strongly depend on the temperature. With increased temperature, viscosities of aqueous reline and ethaline solutions decrease exponentially, and thus, the self-diffusivities and ionic conductivities increase. The effect of water on the transport properties become less pronounced at high temperatures. Temperature does not significantly influence the RDFs and HB networks.

■ ASSOCIATED CONTENT

Supporting Information

The Supporting Information is available free of charge at https://pubs.acs.org/doi/10.1021/acs.jpcb.9b09729.

Force field parameters, tables with raw data for the calculated properties, and additional figures (PDF)

Input and data files for LAMMPS for both aqueous reline and ethaline solutions (ZIP)

DOI: 10.1021/acs.jpcb.9b09729
J. Phys. Chem. B 2019, 123, 11014−11025

AUTHOR INFORMATION

Corresponding Author

*E-mail: o.moultos@tudelft.nl. Phone: +31 (0)15 27 81307.

ORCID

Alper T. Celebi: 0000-0001-7727-194X
Thijs J. H. Vlugt: 0000-0003-3059-8712
Othonas A. Moultos: 0000-0001-7477-9684

Notes

The authors declare no competing financial interest.

ACKNOWLEDGMENTS

This work was sponsored by NWO Exacte Wetenschappen (Physical Sciences) for the use of supercomputer facilities, with financial support from the Nederlandse Organisatie voor Wetenschappelijk Onderzoek. T.J.H.V. acknowledges NWO-CW (Chemical Sciences) for a VICI grant.

REFERENCES

(1) Welton, T. Room-temperature Ionic Liquids. Solvents for Synthesis and Catalysis. *Chem. Rev.* **1999**, *99*, 2071−2084.
(2) Ghandi, K. Review of Ionic Liquids, Their Limits and Applications. *Green Sustain. Chem.* **2014**, *04*, 44.
(3) Kirchhoff, M. M. Promoting Green Engineering through Green Chemistry. *Environ. Sci. Technol.* **2003**, *37*, 5349−5353.
(4) Paiva, A.; Craveiro, R.; Aroso, I.; Martins, M.; Reis, R. L.; Duarte, A. R. C. Natural Deep Eutectic Solvents−Solvents for the 21st Century. *ACS Sustain. Chem. Eng.* **2014**, *2*, 1063−1071.
(5) Brennecke, J. F.; Maginn, E. J. Ionic Liquids: Innovative Fluids for Chemical Processing. *AIChE J.* **2001**, *47*, 2384−2389.
(6) Marsh, K. N.; Boxall, J. A.; Lichtenthaler, R. Room Temperature Ionic Liquids and Their Mixtures—A Review. *Fluid Phase Equilib.* **2004**, *219*, 93−98.
(7) Aparicio, S.; Atilhan, M.; Karadas, F. Thermophysical Properties of Pure Ionic Liquids: Review of Present Situation. *Ind. Eng. Chem. Res.* **2010**, *49*, 9580−9595.
(8) Ramdin, M.; de Loos, T. W.; Vlugt, T. J. H. State-of-the-art of CO2 Capture with Ionic Liquids. *Ind. Eng. Chem. Res.* **2012**, *51*, 8149−8177.
(9) Zhang, Q.; De Oliveira Vigier, K.; Royer, S.; Jérôme, F. Deep Eutectic Solvents: Syntheses, Properties and Applications. *Chem. Soc. Rev.* **2012**, *41*, 7108−7146.
(10) Craveiro, R.; Aroso, I.; Flammia, V.; Carvalho, T.; Viciosa, M. T.; Dionísio, M.; Barreiros, S.; Reis, R. L.; Duarte, A. R. C.; Paiva, A. Properties and Thermal Behavior of Natural Deep Eutectic Solvents. *J. Mol. Liq.* **2016**, *215*, 534−540.
(11) Liu, Y.; Friesen, J. B.; McAlpine, J. B.; Lankin, D. C.; Chen, S.-N.; Pauli, G. F. Natural Deep Eutectic Solvents: Properties, Applications, and Perspectives. *J. Nat. Prod.* **2018**, *81*, 679−690.
(12) Smith, E. L.; Abbott, A. P.; Ryder, K. S. Deep Eutectic Solvents (DESs) and Their Applications. *Chem. Rev.* **2014**, *114*, 11060−11082.
(13) Gu, C. D.; Xu, X. J.; Tu, J. P. Fabrication and Wettability of Nanoporous Silver Film on Copper from Choline Chloride-based Deep Eutectic Solvents. *J. Phys. Chem. C* **2010**, *114*, 13614−13619.
(14) Abbott, A. P.; Capper, G.; McKenzie, K. J.; Ryder, K. S. Electrodeposition of Zinc−Tin Alloys from Deep Eutectic Solvents based on Choline Chloride. *J. Electroanal. Chem.* **2007**, *599*, 288−294.
(15) Ge, X.; Gu, C. D.; Lu, Y.; Wang, X. L.; Tu, J. P. A Versatile Protocol for the Ionothermal Synthesis of Nanostructured Nickel Compounds as Energy Storage Materials from a Choline Chloride-based Ionic Liquid. *J. Mater. Chem. A* **2013**, *1*, 13454−13461.
(16) Wei, L.; Fan, Y.-J.; Tian, N.; Zhou, Z.-Y.; Zhao, X.-Q.; Mao, B.-W.; Sun, S.-G. Electrochemically Shape-Controlled Synthesis in Deep Eutectic Solvents A New Route to Prepare Pt Nanocrystals Enclosed by High-Index Facets with High Catalytic Activity. *J. Phys. Chem. C* **2012**, *116*, 2040−2044.
(17) Florindo, C.; Branco, L. C.; Marrucho, I. M. Development of Hydrophobic Deep Eutectic Solvents for Extraction of Pesticides from Aqueous Environments. *Fluid Phase Equilib.* **2017**, *448*, 135−142.
(18) van Osch, D. J. G. P.; Parmentier, D.; Dietz, C. H. J. T.; van den Bruinhorst, A.; Tuinier, R.; Kroon, M. C. Removal of Alkali and Transition Metal Ions from Water with Hydrophobic Deep Eutectic Solvents. *Chem. Commun.* **2016**, *52*, 11987−11990.
(19) Sharma, M.; Mukesh, C.; Mondal, D.; Prasad, K. Dissolution of α-chitin in Deep Eutectic Solvents. *RSC Adv.* **2013**, *3*, 18149−18155.
(20) Dou, J.; Zhao, Y.; Yin, F.; Li, H.; Yu, J. Mechanistic Study of Selective Absorption of NO in Flue Gas using EG-TBAB Deep Eutectic Solvents. *Environ. Sci. Technol.* **2018**, *53*, 1031−1038.
(21) Steichen, M.; Thomassey, M.; Siebentritt, S.; Dale, P. J. Controlled Electrodeposition of Cu−Ga from a Deep Eutectic Solvent for Low Cost Fabrication of CuGaSe 2 Thin Film Solar Cells. *Phys. Chem. Chem. Phys.* **2011**, *13*, 4292−4302.
(22) Haerens, K.; Matthijs, E.; Chmielarz, A.; Van der Bruggen, B. The Use of Ionic Liquids based on Choline Chloride for Metal Deposition: A Green Alternative? *J. Environ. Manage.* **2009**, *90*, 3245−3252.
(23) Abbott, A. P.; Cullis, P. M.; Gibson, M. J.; Harris, R. C.; Raven, E. Extraction of Glycerol from Biodiesel into a Eutectic Based Ionic Liquid. *Green Chem.* **2007**, *9*, 868−872.
(24) Abbott, A. P.; Ahmed, E. I.; Harris, R. C.; Ryder, K. S. Evaluating Water Miscible Deep Eutectic Solvents (DESs) and Ionic Liquids as Potential Lubricants. *Green Chem.* **2014**, *16*, 4156−4161.
(25) Sheu, C.-Y.; Lee, S.-F.; Lii, K.-H. Ionic Liquid of Choline Chloride/Malonic Acid as a Solvent in the Synthesis of Open-framework Iron Oxalatophosphates. *Inorg. Chem.* **2006**, *45*, 1891−1893.
(26) Yadav, A.; Trivedi, S.; Rai, R.; Pandey, S. Densities and Dynamic Viscosities of (Choline Chloride+ Glycerol) Deep Eutectic Solvent and its Aqueous Mixtures in the Temperature Range (283.15−363.15) K. *Fluid Phase Equilib.* **2014**, *367*, 135−142.
(27) Shah, D.; Mjalli, F. S. Effect of Water on the Thermo-physical Properties of Reline: An Experimental and Mlecular Simulation Based Approach. *Phys. Chem. Chem. Phys.* **2014**, *16*, 23900−23907.
(28) Yadav, A.; Pandey, S. Densities and Ciscosities of (Choline Chloride+ Urea) Deep Eutectic Solvent and its Aqueous Mixtures in the Temperature Range 293.15 K to 363.15 K. *J. Chem. Eng. Data* **2014**, *59*, 2221−2229.
(29) Yadav, A.; Kar, J. R.; Verma, M.; Naqvi, S.; Pandey, S. Densities of Aqueous Mixtures of (Choline Chloride+ Ethylene Glycol) and (Choline Chloride+ Malonic Acid) Deep Eutectic Solvents in Temperature Range 283.15−363.15 K. *Thermochim. Acta* **2015**, *600*, 95−101.
(30) Leron, R. B.; Li, M.-H. High-pressure Density Measurements for Choline Chloride: Urea Deep Eutectic Solvent and its Aqueous Mixtures at T=(298.15 to 323.15) K and up to 50 MPa. *J. Chem. Thermodyn.* **2012**, *54*, 293−301.
(31) Leron, R. B.; Li, M.-H. High-Pressure Volumetric Properties of Choline Chloride−Ethylene Glycol based Deep Eutectic Solvent and its Mixtures with Water. *Thermochim. Acta* **2012**, *546*, 54−60.
(32) Shekaari, H.; Zafarani-Moattar, M. T.; Mohammadi, B. Thermophysical Characterization of Aqueous Deep Eutectic Solvent (Choline Chloride/Urea) Solutions in Full Ranges of Concentration at T=(293.15−323.15) K. *J. Mol. Liq.* **2017**, *243*, 451−461.
(33) Ciocirlan, O.; Croitoru, O.; Iulian, O. Viscosity of Binary Mixtures of 1-ethyl-3-methylimidazolium tetrafluoroborate ionic liquid with four organic solvents. *J. Chem. Thermodyn.* **2016**, *101*, 285−292.
(34) Atashrouz, S.; Zarghampour, M.; Abdolrahimi, S.; Pazuki, G.; Nasernejad, B. Estimation of the Viscosity of Ionic Liquids Containing Binary Mixtures Based on the Eyring's Theory and a Modified Gibbs Energy Model. *J. Chem. Eng. Data* **2014**, *59*, 3691−3704.
(35) Mjalli, F. S.; Mousa, H. Viscosity of Aqueous Ionic Liquids Analogues as a Function of Water Content and Temperature. *Chin. J. Chem. Eng.* **2017**, *25*, 1877−1883.

DOI: 10.1021/acs.jpcb.9b09729
J. Phys. Chem. B 2019, 123, 11014−11025

(36) Fang, S.; He, C.-H. A New One Parameter Viscosity Model for Binary Mixtures. *AIChE J.* **2011**, *57*, 517−524.
(37) Perkins, S. L.; Painter, P.; Colina, C. M. Experimental and Computational Studies of Choline Chloride-based Deep Eutectic Solvents. *J. Chem. Eng. Data* **2014**, *59*, 3652−3662.
(38) Perkins, S. L.; Painter, P.; Colina, C. M. Molecular Dynamic Simulations and Vibrational Analysis of an Ionic Liquid Analogue. *J. Phys. Chem. B* **2013**, *117*, 10250−10260.
(39) Zhekenov, T.; Toksanbayev, N.; Kazakbayeva, Z.; Shah, D.; Mjalli, F. S. Formation of Ype III Deep Eutectic Solvents and Effect of Water on Their Intermolecular Interactions. *Fluid Phase Equilib.* **2017**, *441*, 43−48.
(40) Fetisov, E. O.; Harwood, D. B.; Kuo, I.-F. W.; Warrag, S. E. E.; Kroon, M. C.; Peters, C. J.; Siepmann, J. I. First-principles Molecular Dynamics Study of a Deep Eutectic Solvent: Choline Chloride/Urea and its Mixture with Water. *J. Phys. Chem. B* **2018**, *122*, 1245−1254.
(41) Kumari, P.; Shobhna; Kaur, S.; Kashyap, H. K. Influence of Hydration on the Structure of Reline Deep Eutectic Solvent: A Molecular Dynamics Study. *ACS Omega* **2018**, *3*, 15246−15255.
(42) Baz, J.; Held, C.; Pleiss, J.; Hansen, N. Thermophysical Poperties of Glyceline−Water Mixtures Investigated by Molecular Modelling. *Phys. Chem. Chem. Phys.* **2019**, *21*, 6467−6476.
(43) Wang, J.; Wolf, R. M.; Caldwell, J. W.; Kollman, P. A.; Case, D. A. Development and Testing of a General Amber Force Field. *J. Comput. Chem.* **2004**, *25*, 1157−1174.
(44) Sun, H.; Li, Y.; Wu, X.; Li, G. Theoretical Study on the Structures and Properties of Mixtures of Urea and Choline Chloride. *J. Mol. Model.* **2013**, *19*, 2433−2441.
(45) Mark, P.; Nilsson, L. Structure and Dynamics of the TIP3P, SPC, and SPC/E Water Models at 298 K. *J. Phys. Chem. A* **2001**, *105*, 9954−9960.
(46) Tsimpanogiannis, I. N.; Moultos, O. A.; Franco, L. F. M.; Spera, M. B. d. M.; Erdős, M.; Economou, I. G. Self-diffusion Coefficient of Bulk and Confined Water: A Critical Review of Classical Molecular Simulation Studies. *Mol. Simul.* **2019**, *45*, 425−453.
(47) Orozco, G. A.; Moultos, O. A.; Jiang, H.; Economou, I. G.; Panagiotopoulos, A. Z. Molecular Simulation of Thermodynamic and Transport Properties for the H2O+ NaCl System. *J. Chem. Phys.* **2014**, *141*, 234507.
(48) Celebi, A. T.; Beskok, A. Molecular and Continuum Transport Perspectives on Electroosmotic Slip Flows. *J. Phys. Chem. C* **2018**, *122*, 9699−9709.
(49) Martínez, L.; Andrade, R.; Birgin, E. G.; Martínez, J. M. PACKMOL: A Package for Building Initial Configurations for Molecular Dynamics Simulations. *J. Comput. Chem.* **2009**, *30*, 2157−2164.
(50) Plimpton, S. Fast Parallel Algorithms for Short-range Molecular Dynamics. *J. Comput. Phys.* **1995**, *117*, 1−19.
(51) Plimpton, S.; Pollock, R.; Stevens, M. Particle-Mesh Ewald and rRESPA for Parallel Molecular Dynamics Simulations. *Proceedings of the Eighth SIAM Conference on Parallel Processing for Scientific Computing, Minneapolis, MN*, 1997; pp 1−13.
(52) Allen, M. P.; Tildesley, D. J. *Computer Simulation of Liquids*, 2nd ed.; Oxford University Press: New York, USA, 2017.
(53) Miyamoto, S.; Kollman, P. A. Settle: An Analytical Version of the SHAKE and RATTLE Algorithm for Rigid Water Models. *J. Comput. Chem.* **1992**, *13*, 952−962.
(54) Jamali, S. H.; Wolff, L.; Becker, T. M.; de Groen, M.; Ramdin, M.; Hartkamp, R.; Bardow, A.; Vlugt, T. J. H.; Moultos, O. A. OCTP: A Tool for On-the-fly Calculation of Transport Properties of Fluids with the Order-n Algorithm in LAMMPS. *J. Chem. Inf. Model.* **2019**, *59*, 1290−1294.
(55) Dubbeldam, D.; Ford, D. C.; Ellis, D. E.; Snurr, R. Q. A New Perspective on the Order-n Algorithm for Computing Correlation Functions. *Mol. Simul.* **2009**, *35*, 1084−1097.
(56) Frenkel, D.; Smit, B. *Understanding Molecular Simulation: from Algorithms to Applications*, 1st ed.; Elsevier, 2001.
(57) Ganguly, P.; van der Vegt, N. F. A. Convergence of Sampling Kirkwood−Buff Integrals of Aqueous Solutions with Molecular Dynamics Simulations. *J. Chem. Theory Comput.* **2013**, *9*, 1347−1355.
(58) Milzetti, J.; Nayar, D.; van der Vegt, N. F. A. Convergence of Kirkwood−Buff Integrals of Ideal and Nonideal Aqueous Solutions Using Molecular Dynamics Simulations. *J. Phys. Chem. B* **2018**, *122*, 5515−5526.
(59) Dawass, N.; Krüger, P.; Schnell, S. K.; Simon, J.-M.; Vlugt, T. J. H. Kirkwood-Buff Integrals from Molecular Simulation. *Fluid Phase Equilib.* **2019**, *486*, 21−36.
(60) Humphrey, W.; Dalke, A.; Schulten, K. VMD: Visual Molecular Dynamics. *J. Mol. Graph.* **1996**, *14*, 33−38.
(61) Ciocirlan, O.; Iulian, O.; Croitoru, O. Effect of Temperature on the Physico-chemical Properties of Three Ionic Liquids Containing Choline Chloride. *Rev. Chim (Bucharest)* **2010**, *61*, 721−723.
(62) Touloukian, Y. S.; Kirby, R.; Taylor, R.; Desai, P. *Thermal Expansion: Metallic Elements and Alloys*; IFI/Plenum: New York, 1975; Vol. 2.
(63) Tazi, S.; Boţan, A.; Salanne, M.; Marry, V.; Turq, P.; Rotenberg, B. Diffusion Coefficient and Shear Viscosity of Rigid Water Models. *J. Phys. Condens. Matter* **2012**, *24*, 284117.
(64) Medina, J. S.; Prosmiti, R.; Villarreal, P.; Delgado-Barrio, G.; Winter, G.; González, B.; Alemán, J. V.; Collado, C. Molecular Dynamics Simulations of Rigid and Flexible Water Models: Temperature Dependence of Viscosity. *Chem. Phys.* **2011**, *388*, 9−18.
(65) Yeh, I.-C.; Hummer, G. System-size Dependence of Diffusion Coefficients and Viscosities from Molecular Dynamics Simulations with Periodic Boundary Conditions. *J. Phys. Chem. B* **2004**, *108*, 15873−15879.
(66) Jamali, S. H.; Wolff, L.; Becker, T. M.; Bardow, A.; Vlugt, T. J. H.; Moultos, O. A. Finite-size Effects of Binary Mutual Diffusion Coefficients from Molecular Dynamics. *J. Chem. Theory Comput.* **2018**, *14*, 2667−2677.
(67) D'Agostino, C.; Harris, R. C.; Abbott, A. P.; Gladden, L. F.; Mantle, M. D. Molecular Motion and Ion Diffusion in Choline Chloride Based Deep Eutectic Solvents Studied by 1 H Pulsed Field Gradient NMR Spectroscopy. *Phys. Chem. Chem. Phys.* **2011**, *13*, 21383−21391.
(68) D'Agostino, C.; Gladden, L. F.; Mantle, M. D.; Abbott, A. P.; Essa, I. A.; Al-Murshedi, A. Y.; Harris, R. C. Molecular and Ionic Diffusion in Aqueous−Deep Eutectic Solvent Mixtures: Probing Inter-molecular Interactions using PFG NMR. *Phys. Chem. Chem. Phys.* **2015**, *17*, 15297−15304.
(69) Holz, M.; Heil, S. R.; Sacco, A. Temperature-dependent Self-diffusion Coefficients of Water and Six Selected Molecular Liquids for Calibration in Accurate 1H NMR PFG Measurements. *Phys. Chem. Chem. Phys.* **2000**, *2*, 4740−4742.
(70) Mjalli, F. S.; Ahmed, O. U. Physical Properties and Intermolecular Interaction of Eutectic Solvents Binary Mixtures: Reline and Ethaline. *Asia Pac. J. Chem. Eng.* **2016**, *11*, 549−557.
(71) Humbert, M. T.; Zhang, Y.; Maginn, E. J. PyLAT: Python LAMMPS Analysis Tools. *J. Chem. Inf. Model.* **2019**, *59*, 1301−1305.
(72) Agieienko, V.; Buchner, R. Densities, Viscosities, and Electrical Conductivities of Pure Anhydrous Reline and Its Mixtures with Water in the Temperature Range (293.15 to 338.15) K. *J. Chem. Eng. Data* **2019**, *64*, 4763−4774.
(73) Mjalli, F. S.; Ahmed, O. U. Ethaline and Glyceline Binary Eutectic Mixtures: Characteristics and Intermolecular Interactions. *Asia-Pac. J. Chem. Eng.* **2017**, *12*, 313−320.
(74) Tu, K.-M.; Ishizuka, R.; Matubayasi, N. Spatial-decomposition Analysis of Electrical Conductivity in Concentrated Electrolyte Solution. *J. Chem. Phys.* **2014**, *141*, 044126.
(75) Hammond, O. S.; Bowron, D. T.; Edler, K. J. Liquid Structure of the Choline Chloride-Urea Deep Eutectic Solvent (Reline) from Neutron Diffraction and Atomistic Modelling. *Green Chem.* **2016**, *18*, 2736−2744.
(76) Gao, Q.; Zhu, Y.; Ji, X.; Zhu, W.; Lu, L.; Lu, X. Effect of Water Concentration on the Microstructures of Choline Chloride/Urea (1:2)/Water Mixture. *Fluid Phase Equilib.* **2018**, *470*, 134−139.

DOI: 10.1021/acs.jpcb.9b09729
J. Phys. Chem. B 2019, 123, 11014−11025

(77) Kohagen, M.; Brehm, M.; Lingscheid, Y.; Giernoth, R.; Sangoro, J.; Kremer, F.; Naumov, S.; Iacob, C.; Kärger, J.; Valiullin, R.; Kirchner, B. the others, How Hydrogen Bonds Influence the Mobility of Imidazolium-based Ionic Liquids. A Combined Theoretical and Experimental Study of 1-n-butyl-3-methylimidazolium Bromide. *J. Phys. Chem. B* **2011**, *115*, 15280−15288.
(78) Zhao, W.; Leroy, F.; Heggen, B.; Zahn, S.; Kirchner, B.; Balasubramanian, S.; Müller-Plathe, F. Are There Stable Ion-pairs in Room-temperature Ionic Liquids? Molecular Dynamics Simulations of 1-n-butyl-3-methylimidazolium hexafluorophosphate. *J. Am. Chem. Soc.* **2009**, *131*, 15825−15833.
(79) Hammond, O. S.; Bowron, D. T.; Edler, K. J. The Effect of Water upon Deep Eutectic Solvent Nanostructure: An Unusual Transition from Ionic Mixture to Aqueous Solution. *Angew. Chem.* **2017**, *56*, 9782−9785.
(80) Stefanovic, R.; Ludwig, M.; Webber, G. B.; Atkin, R.; Page, A. J. Nanostructure, Hydrogen Bonding and Rheology in Choline Chloride Deep Eutectic Solvents as a Function of the Hydrogen Bond Donor. *Phys. Chem. Chem. Phys.* **2017**, *19*, 3297−3306.
(81) Döpke, M. F.; Lutzenkirchen, J.; Moultos, O. A.; Siboulet, B.; Dufrêche, J.-F.; Padding, J. T.; Hartkamp, R. Preferential Adsorption in Mixed Electrolytes Confined by Charged Amorphous Silica. *J. Phys. Chem. C* **2019**, *123*, 16711.
(82) Kelkar, M. S.; Shi, W.; Maginn, E. J. Determining the Accuracy of Classical Force Fields for Ionic Liquids: Atomistic Simulation of the Thermodynamic and Transport Properties of 1-ethyl-3-methylimidazolium ethylsulfate ([emim][EtSO4]) and its Mixtures with Water. *Ind. Eng. Chem. Res.* **2008**, *47*, 9115−9126.
(83) Salanne, M. Simulations of Room Temperature Ionic Liquids: From Polarizable to Coarse-grained Force Fields. *Phys. Chem. Chem. Phys.* **2015**, *17*, 14270−14279.
(84) Jiang, H.; Mester, Z.; Moultos, O. A.; Economou, I. G.; Panagiotopoulos, A. Z. Thermodynamic and Transport Properties of H2O+ NaCl from Polarizable Force Fields. *J. Chem. Theory Comput.* **2015**, *11*, 3802−3810.
(85) Hunt, P. A. The Simulation of Imidazolium-based Ionic Liquids. *Mol. Simul.* **2006**, *32*, 1−10.

DOI: 10.1021/acs.jpcb.9b09729
J. Phys. Chem. B 2019, 123, 11014−11025